Cell. Mol. Life Sci. 63 (2006) 505–514
1420-682X/06/040505-10
DOI 10.1007/s00018-005-5472-x
© Birkhäuser Verlag, Basel, 2006

Cellular and Molecular Life Sciences

Research Article

On the self-association potential of transmembrane tight junction proteins

I. E. Blasig[a, *, †], L. Winkler[a, †], B. Lassowski[a], S. L. Mueller[a], N. Zuleger[a], E. Krause[a], G. Krause[a], K. Gast[b], M. Kolbe[c] and J. Piontek[a]

[a] Forschungsinstitut für Molekulare Pharmakologie, Robert-Rössle-Str. 10, 13125 Berlin (Germany),
Fax: +49 30 94793 244/243, e-mail: iblasig@fmp-berlin.de
[b] Institute for Biochemistry and Biology, Universität Potsdam (Germany)
[c] Max-Planck-Institute for Infection Biology, Berlin (Germany)

Received 6 October 2005; received after revision 14 December 2005; accepted 27 December 2005
Online First 2 February 2006

Abstract. Tight junctions seal intercellular clefts via membrane-related strands, hence, maintaining important organ functions. We investigated the self-association of strand-forming transmembrane tight junction proteins. The regulatory tight junction protein occludin was differently tagged and cotransfected in eucaryotic cells. These occludins colocalized within the plasma membrane of the same cell, coprecipitated and exhibited fluorescence resonance energy transfer. Differently tagged strand-forming claudin-5 also colocalized in the plasma membrane of the same cell and showed fluorescence resonance energy transfer. This demonstrates self-association in intact cells both of occludin and claudin-5 in one plasma membrane. In search of dimerizing regions of occludin, dimerization of its cytosolic C-terminal coiled-coil domain was identified. In claudin-5, the second extracellular loop was detected as a dimer. Since the transmembrane junctional adhesion molecule also is known to dimerize, the assumption that homodimerization of transmembrane tight junction proteins may serve as a common structural feature in tight junction assembly is supported.

Keywords. Occludin, claudin-5, tight junction, dimerization, protein-protein interaction.

Tight junctions (TJs) regulate paracellular permeability of endothelia and epithelia. Occludin, claudins and junctional adhesion molecules (JAMs) are unique transmembrane proteins specifically localized in TJs. Together with the membrane-associated zonula occludens protein (ZO) family, the multiprotein assembly of TJs is composed. To date, neither the exact molecular structure of TJ subunits nor the organization principle is known. Defining the architecture of TJs, therefore, is a prerequisite to understanding the barrier function at a molecular level.

Occludin has four transmembrane helices. The end of the cytosolic C terminus folds into a coiled-coil domain, which associates with ZO-1 [1] and might offer oligomerization properties [2, 3]. Disruption of occludin barrier-forming properties is achieved through transfection of occludin mutants without intracellular parts [4], and supports their relevance for TJ arrangement. ZO-1 might, via its scaffolding function, recruit occludin at TJs and regulate its function, since occludin remains diffusely stained at the cell surface of fibroblasts lacking expression of ZO-1 [5]. Claudins also have four transmembrane helices and two extracellular loops. Claudins and occludin are thought to interdigitate intermolecularly in linear strands on one cell to form TJ complexes by sealing with complementary strands on the surface of adjacent cells [6].

Claudins can bind to the PDZ-1 domain [7], JAM to the PDZ-3 domain of ZO-1 [8]. However, exact regions and

* Corresponding author.
† These authors contributed equally to this work.

mechanisms of interaction are not well understood. JAMs comprise a family of immunoglobulin-like proteins with one transmembrane helix and they are suggested to participate in TJ sealing [9]. Crystal structure analysis of JAMs has proposed self-adhesion via a specific extracellular dimerization motif [10].

ZO proteins 1, 2 and 3 are involved in regulating protein assembly at cell-cell contacts [11], differentiation [8], regulation of gene expression and binding to the cytoskeleton [12]. They belong to membrane-associated guanylate kinase homologue proteins (MAGuKs) with a conserved order of PDZ, SH3, GuK domains, acidic and proline-rich regions [11]. As ZO-1 can interact with claudins [7], JAMs [8], occludin and even with itself [1], these interactions have been hypothesized to play a significant role in assembly of the TJ structure. Together with linkage to the cytoskeleton, the associations between cytoplasmic and transmembrane proteins may arrange TJs and modulate the barrier function [13].

The aim of this investigations was to demonstrate and to charcterize self-association of occludin und junction-forming claudins for the full-length proteins in cells, and for selected constructs *in vitro*. Occludin and the strand-forming claudin-5, both with fluorescence tags, showed resonance energy transfer demonstrating homodimerization. Dimerization of the second extracellular loop of claudin-5 was found and can contribute to the self-association as well as dimerization of the C-terminal coiled-coil domain of occludin. Taken together, these and literature data concerning JAMs and ZO-1 support the assumption that dimerization of transmembrane TJ proteins is a new basic priciple to organize the protein ensemble of TJs.

Materials and methods

Cultivation and transfection of cells. HEK-293 cells (human embryonal kidney cell line 239), and Madin-Darby canine kidney (MDCK) cells were cultured in Dulbecco's modified Eagle's medium (DMEM) supplemented with 10% fetal calf serum (FCS), 2 mM L-glutamine, 100 U penicillin, 100 mg/ml streptomycin. Transfection was performed with lipofectamine 2000 (Invitrogen, Karlsruhe, Germany) according to the supplier's recommendations. Three days after transfection, the cells were analyzed.

Cloning of proteins and preparation of expression constructs. If not stated otherwise, mouse sequences were cloned via *Bam*HI and *Sal*I sites N-terminally fused with maltose-binding protein (MBP; vector pMAL-c2X; NEB, Schwalbach, Germany). Occludin and parts thereof were obtained by RT-PCR [14]. To generate C-terminally His_6- and FLAG-tagged full-length occludin, the respective cDNA was amplified by PCR using reverse primers including codons for His_6 and FLAG, respectively. The PCR products were ligated in pcDNA3.11 vector using *Bam*H1 and *Pme*I restriction sites (Fermentas MBI, St. Leon Rot, Germany). A segment of the claudin-5 cDNA corresponding to amino acids 141–161 was amplified from the plasmid pGTCL-5 (kind gift of Dr. M. Furuse, Kyoto, Japan) via PCR and ligated into the multiple cloning site of the expression vector pMAL-c2X. For generating a plasmid encoding the fusion protein of claudin-5 and C-terminal cyan/yellow fluorescent protein (CFP/YFP), full-length claudin-5 was amplified by PCR using pGTCL-5 as template, forward and reverse primers containing *Sal*I and *Bam*HI restriction sites, respectively, and then subcloned in the plasmid pECFP-N1/pEYFP-N1 (BD Biosciences, Freiburg, Germany). Claudin-5 containing a FLAG tag at the C terminus was generated by amplifying full-length claudin-5 by PCR using pGTCL-5 as template, forward primer containing a *Sal*I restriction site and a reverse primer containing a sequence encoding the FLAG peptide, stop codon and *Bam*HI restriction site. The product was subcloned in the plasmid pEYFP-N1. Due to the stop codon, the YFP sequence was not part of claudin-5-FLAG. For generating a plasmid encoding the fusion protein of occludin and N-terminal CFP/YFP, full-length occludin was amplified by PCR using occludin in pcDNA3.11 as template, forward and reverse primers containing *Hind*III and *Bam*HI restriction sites, respectively, and then subcloned in the plasmid pECFP-C1/pEYFP-C1 (BD Biosciences, Freiburg, Germany).

Production of proteins and protein determination. MBP-fusion proteins were purified as described elsewhere [1]. To cleave the MBP, 1 µg protease factor Xa (NEB, Beverly Calif.; 25 °C, 16 h) was added per 100 µg MBP-occludin$^{406–521}$ in 2 mM $CaCl_2$. Then, maltose was removed by dialysis (3.5-kDa pore membrane; Serva, Heidelberg, Germany) against 10 mM Tris/HCl pH 7.5, 20 mM NaCl. To separate the cleaved MBP, the dialysate was applied several times to an amylose-resin column. The flowthrough with occludin$^{406–521}$ was collected. The protein concentration was determined using the Lowry assay [15].

Immunocytochemistry and coprecipitation. SDS-PAGE and immunoblotting were performed as described previously [16]. Horseraddish peroxidase (HRP)-conjugated anti-rabbit IgG (immunglobulin G), HRP-conjugated anti-mouse IgG and Cy3-conjugated anti-mouse IgG were from Zytomet, Berlin, Germany; Alexa-Fluor-488-conjugated anti-rabbit IgG antibodies were from Molecular Probes, Eugene, Ore., USA; anti-His_6- and anti-FLAG-tag antibodies were from Sigma, Taufkirchen, Germany. Anti-GFP antibody preparation 01 (generous gift of R. Schülein, FMP, Berlin, Germany) was used for detection of CFP and YFP. For immunocytochemistry, cells were washed with PBS, fixed with acetone (5 min, 4 °C),

washed again with ethanol (1 min, 4 °C) and PBS (1 min, 4 °C), soaked in blocking solution (1% bovine serum albumin and 0.05% Tween 20 in PBS; BS) for 10 min and then incubated with the first primary antibody in BS for 1 h. After washing (5×2 min BS), samples were incubated with the second primary antibody in BS for 1 h, washed (5×2 min BS), incubated with secondary antibodies for 30 min in BS, and washed (5×2 min BS). Cells were examined using an LSM 510 confocal microscope (Zeiss, Jena, Germany).

For coprecipitation assays, transfected HEK-293 cells, in 35-mm dishes, were washed with PBS, scraped off in PBS, and collected (5 min, 300 g). Cells were resuspended in lysis buffer (LS: 5 mM imidazol, 0.75% Triton X-100 in PBS, supplemented with EDTA-free protease inhibitor cocktail according to Roche, Mannheim, Germany), incubated for 10 min on ice and centrifuged (10 min, 20,000 g, 4 °C). The supernatant (lysate) was incubated with Ni-nitrilotriacetic acid-agarose-beads (Qiagen, Hilden, Germany) for 90 min on a shaker at 4 °C. The beads were collected by centrifugation (2 min, 3,000 g, 4 °C). The supernatant (unbound fraction) was aspirated and the beads washed (4× LS containing 20 mM imidazol). Bound proteins were eluted with LS containing 250 mM imidazol (eluate).

Fluorescence resonance energy transfer analysis. For fluorescence resonance energy transfer (FRET) acceptor photobleaching [17], HEK-293 cells were cotransfected with plasmids encoding claudin-5-CFP and claudin-5-YFP, claudin-5-CFP and YFP-aquaporin-1 (gift of S. Tsunoda, Berlin, Germany), CFP and claudin-5-YFP, claudin-5-CFP and corticotropin releasing factor receptor 1 **(**CRFR)-YFP (gift of O. Krätke, Berlin, Germany), CFP-occludin and YFP-occludin, CFP and YFP, or CFP-YFP tandem (gift of O. Krätke). After 3 days, cells were transferred into DMEM without phenol red and 10 mM HEPES pH 7.5. Cells were analyzed with a confocal microscope. CFP and YFP were excited at 458 and 514 nm, respectively. Fluorescence emitted from CFP and YFP was detected from 462.6 to 494.7 nm and 526.8 to 633.8 nm, respectively. Cells exhibiting CFP and YFP fluorescence were used. Photobleaching of YFP was performed using 30–40 pulses of the 514-nm argon laser line at 100% intensity. Before and after acceptor bleaching, CFP intensity images were recorded to calculate changes in donor fluorescence in the area of cell-cell contacts. FRET efficiency (E_F) was calculated as $E_F = (I_A - I_B)\times 100/I_A$, where I_B and I_A refer to the CFP intensity before and after the photobleaching, respectively. The pairs claudin-5/aquaporin-1 and claudin-5/CRFR-1 were chosen as controls, as these proteins represent any transmembrane protein and were not expected to interact with each other. Aquaporin-1 and CRFR-1 are normally not expressed in detectable amounts in HEK-293 cells. [18, 19]; after transfection, they are predominantly distributed throughout the plasma membrane [20].

Size-exclusion chromatography. Analytical size-exclusion chromatography was performed on a Shimadzu HPLC system (LC-10AS pump, SPD-10A UV detector; Shimadzu, Tokyo, Japan) using PBS (Biochrom, Berlin, Germany) containing 1 mM EDTA at 22 °C. For purified MBP-claudin-$5^{141–161}$, MBP and occludin, a Superdex 200 HR 10/30 column (Amersham Biosciences, Uppsala, Sweden) was used. Samples and buffers were filtered (0.45 µm); standards and samples were injected in a volume of 50 µl. The flow rate was 0.5 ml/min. Protein concentrations were monitored at 214 or 280 nm, using standards from a low-weight calibration kit (Amersham Biosciences).

Dynamic light scattering and static light-scattering measurements. These were performed simultaneously at a scattering angle of 90° with a laboratory-built apparatus, presently equipped with a diode-pumped, continuous-wave laser Millennia IIs (Spectra-Physics, Darmstadt, Germany) and a high-quantum-yield avalanche photodiode as described elsewhere [21]. The translational diffusion coefficient D was obtained from the measured autocorrelation functions using the program CONTIN [22]. The diffusion coefficients were converted into Stokes radii via the Stokes-Einstein equation $R_S = k_B T/(6\pi\eta_0 D)$, were k_B is Boltzmann's constant, T is the temperature in Kelvin and η_0 is the solvent viscosity. Molar masses were estimated from the relative scattering intensities using toluene as a reference sample and applying a refractive index increment (dn/dc) = 0.19 ml/g. Solutions were filtered (0.1-µm Anotop filters; Whatman, London, UK) into 80 µl rectangular fluorescence cells.

Mass spectrometry. Matrix-assisted laser desorption/ionization mass spectrometry (MALDI-MS) was performed on a Voyager-DE STR BioSpectrometry Workstation MALDI-TOF mass spectrometer (Perseptive Biosystems, Framingham, Mass.). Samples were prepared with a sinapinic acid matrix and measured in the linear mode at an acceleration voltage of 25 kV. Each spectrum obtained was the mean of 256 laser shots. One microlitre effluate from size-exclusion chromatography was mixed with 1 µl of sinapic acid solution consisting of 10 mg of the matrix dissolved in 1 ml of 0.3% trifluoroacetic acid in acetonitrile-water (1:1, v/v). One microlitre of the resulting mixture was applied to the sample plate. Samples were air-dried at ambient temperature (24 °C).

Statistics. Data represent means ± SE; statistical analysis was performed by one-way ANOVA with a subsequent unpaired t test, where $p < 0.01$ was defined as significant.

Results

First, the colocalization of different occludin molecules was visualized. Figure 1a–c shows fluorescence images of living and confluent MDCK cells, cotransfected with CFP-occludin and YFP-occludin. As evident from the merge, both fusion proteins colocalized in the plasma membrane of the same cell, even in areas which were attached to non-transfected cells, indicating proper targeting and potential interaction of the fusion proteins.

To investigate whether occludin physically interacts with itself in one plasma membrane, a FRET assay was applied. TJ-free HEK-293 cells were used to analyze the interactions independently of the influence of endogenous TJs. Figure 1d–f shows fluorescence images of living HEK cells, cotransfected with CFP-occludin and YFP-occludin. Both fusion proteins were enriched at contacts between two transfected cells, presumably due to a head-to-head interaction between occludin of the two opposing plasma membranes. This contact area was marked (Fig. 1f, encircled with a red line). The FRET efficiency was determined by comparing the CFP fluorescence in the marked area before and after acceptor (YFP) photobleaching. As controls, we analyzed cells transfected with a CFP-YFP tandem protein, cotransfected with CFP and YFP as well as with claudin-5-CFP and YFP-aquaporin-1. As shown in Figure 1g, the positive control (CFP-YFP tandem protein) reached a high FRET efficiency (30.5 ± 3.4%). The negative controls of protein pairs that should not interact (CFP and YFP, claudin-5-CFP and YFP-aqua-

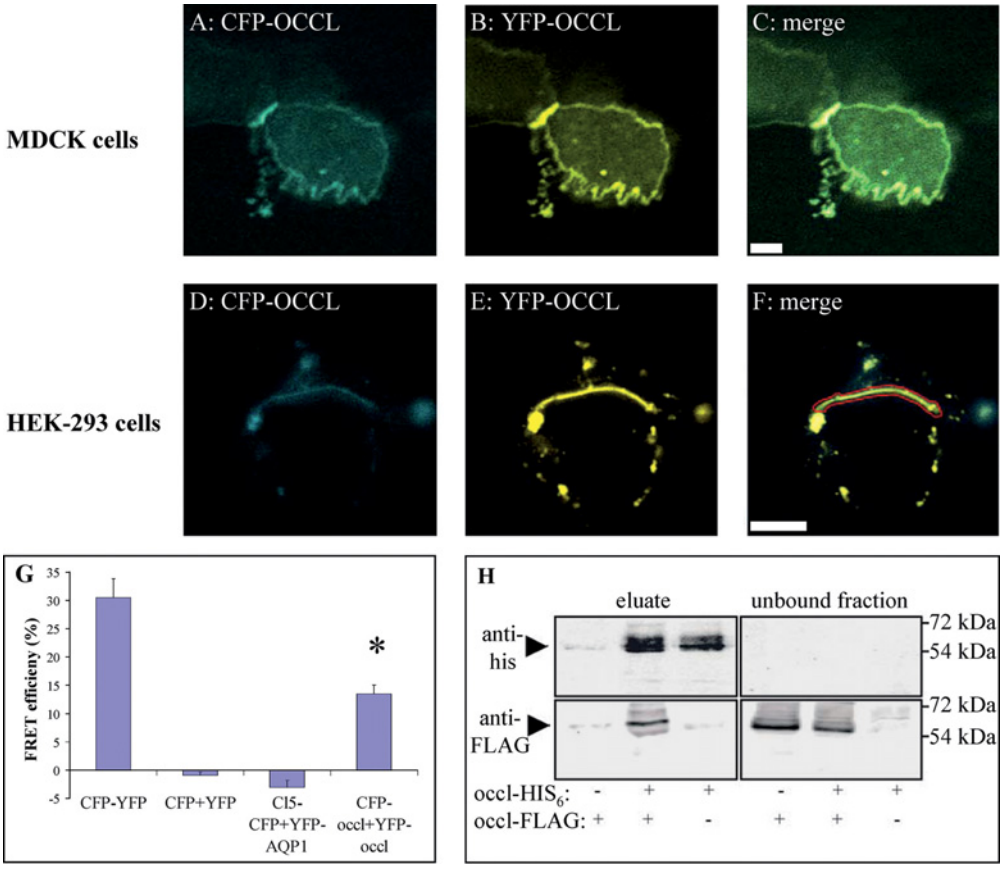

Figure 1. Self-association of occludin in mammalian cells. (*a–c*) Fluorescence image of living MDCK cells, cotransfected with CFP-occludin (*a*, CFP-OCCL) and YFP-occludin (*b*, YFP-OCCL) showing plasma membrane localization and colocalization of the two fusion proteins in epithelial cells (*c*). (*d–f*) Fluorescence image of living HEK-293 cells, CFP-occludin (*d*) and YFP-occludin (*e*), showing enrichment at contacts between two cells (*f*, red area) and colocalization of the two fusion proteins. Bar, 5 µm. (*g*) FRET analysis using acceptor photobleaching. The cell-cell contact area was marked (*f*, red) and the respective CFP fluorescence in this area was determined before and after YFP photobleaching. The FRET efficiencies were calculated from HEK-293 cells expressing a CFP-YFP fusion protein, CFP and YFP, claudin-5-CFP (CL5-CFP) and YFP-aquaporin-1 (Aqp-1), or CFP-occl and YFP-occl. The efficiency for CFP-occl/YFP-occl was significantly higher than for CFP + YFP and claudin-5-CFP + YFP-aquaporin-1, indicating that occludin is specifically self-associating within one plasma membrane. Data are means ± SE, n = 20 cells in each group, *p < 0.01 compared to the two middle columns. (*h*) Coprecipitaion of occludin-FLAG by occludin-His_6 using Ni-NTA-resin demonstrates binding of occludin-FLAG to occludin-His_6 in cells. Extracts from HEK-293 cells cotransfected with occludin-FLAG and occludin-His_6 were incubated with Ni-NTA-resin to isolate occludin-His_6 specifically. The resulting bound and unbound fractions were analyzed via immunoblotting by means of mouse anti-FLAG or anti-His_6 antibodies. Arrowhead indicate the molecular weight of occludin (65 kDa).

porin-1) showed no considerable signal (–0.9 ± 0.6% and –3.0 ± 1.2%, respectively). Cells coexpressing CFP-occludin and YFP-occludin showed a significantly higher (13.5 ± 1.6%) FRET efficiency than the negative controls ($p > 0.01$, $n = 20$ each, mean ± SE). These data demonstrate a close spatial association of two occludin molecules within one plasma membrane, because a FRET from the CFP tag of one occludin to the YFP tag of another one is only possible within one plasma membrane but not between those of two opposing cells because the distance is much larger than necessary for FRET (≤6nm [23]).

The occludin self-assoziation revealed by FRET was verified by coprecipitation. Immunoblotting of extracts from HEK-293 cells cotransfected with occludin-His_6 and occludin-FLAGc, obtained after specific isolation of His_6 by means of Ni-NTA resin, demonstrated coprecipitation of the 65-kDa protein occludin-FLAG along 65-kDa occludin-His_6 (Fig. 1h, eluate: middle lanes). Eluate from cells transfected with occludin-His_6 only showed immunoreactivity with anti-His_6 antibodies but not with anti-FLAG antibodies (Fig. 1h, third lane). The fractions which did not bind to Ni-NTA resin were free of His_6 immunoreactivity (Fig. 1h, lane 5 and 6) indicating complete removal of occludin-His_6 from cell extracts. Occludin of cells only transfected with occludin-FLAG could not be bound to the Ni-NTA resin and therefore were not traced in the eluate by anti-FLAG antibodies (Fig. 1h, first lane). FLAG immunoreactivity was detectable in unbound fractions from extracts of occludin-FLAG monotransfected cells (Fig. 1h, unbound fraction: lane 4 and 5), demonstrating no binding to the Ni matrix. Taken together, the cell studies document that full-length occludin may bind to itself within the same cell.

In addition, the area and size of occludin self-association were studied. Size-exclusion chromatography of the C-terminal cytosolic tail of occludin, mouse occludin$^{406–521}$ containing predicted α and coiled-coil helices [24], eluted at about 14 and 28 kDa (Fig. 2, upper part). Both peaks were identified as occludin fragments by mass spectrometry. A mass spectrum of the 28-kDa fraction

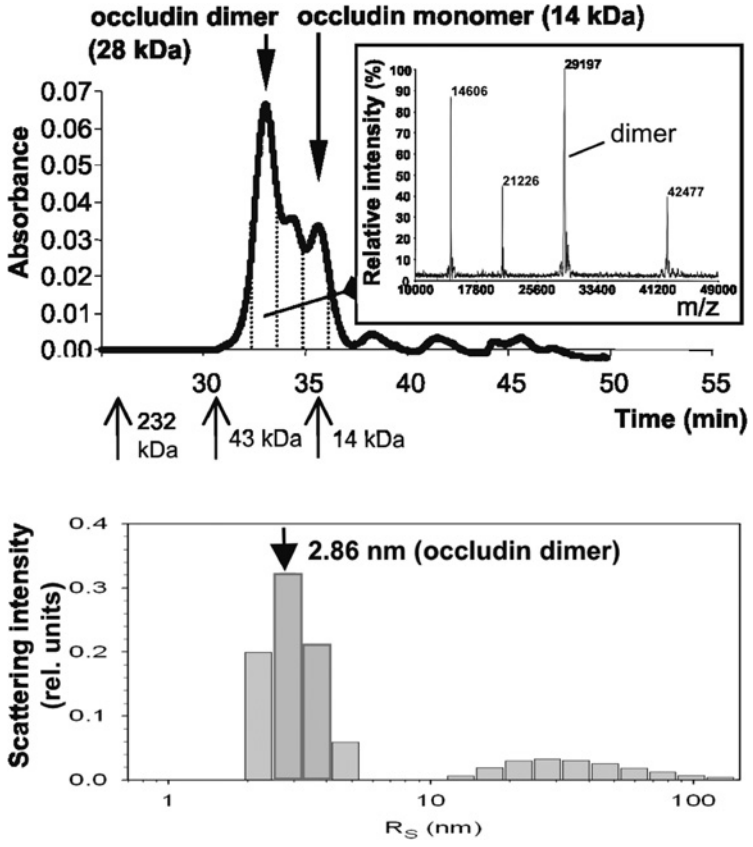

Figure 2. Dimer formation by the coiled-coil domain of occludin (mouse occludin$^{406–521}$). Upper part: size-exclusion chromatography of 0.5 mg/ml mainly shows formation of a dimer. Bold arrows mark peaks of the chromatogram, containing occludin as verified by mass spectrometry. Open arrows indicate molecular weight marker proteins (catalase, 232 kDa; ovalbumin, 43 kDa; ribonuclease, 14 kDa). Inset: mass spectrogram of 28-kDa peak fraction demonstrating predominant existence of the dimer. Lower part: dynamic light scattering of 0.4 mg/ml of occludin$^{406–521}$ in 20 mM NaCl, 1 mM β-mercaptoethanol, 10 mM Tris/HCl pH 7.4. Bars represent the distribution of Stokes radii (R_S) according to the scattered-light intensity. The main peak of bars with an average R_S of 2.86 ± 0.07 nm ($n = 4$; arrow) suggests the existence of predominantly dimeric occludin, since the R_S calculated for the monomer using scaling laws for globular proteins amounted to 1.92 nm. The broad peak between 10 and 100 nm is due to the presence of traces of aggregates.

confirmed the presence of the dimer with m/z 29197, whereas the peak at m/z 14606 represents the monomer. The peaks at m/z 42477 and 21226 correspond to smaller amounts of singly and doubly charged trimer, respectively (inset, Fig. 2 upper part). The cytosolic occludin domain, therefore, exists as a monomer/dimer equilibrium. Immunoblotting of occludin$^{406–521}$ before size-exclusion chromatography using SDS gel electrophoresis under reducing conditions also showed bands at 14 and 28 kDa (data not shown). Dynamic light-scattering studies of occludin$^{406–521}$ in solution yielded the size distribution shown in Figure 2 (lower part). The main peak with Stokes radii between 2 and 4.5 nm and an average radius of about 2.9 nm essentially resulted from dimers. This was substantiated by the average mass of 23±5 kDa calculated for this peak from static light-scattering data. The relatively large width of this peak was probably due to the presence of certain amounts of monomers and a few higher oligomers. The presence of monomers led to an average mass, which is somewhat smaller than the exact mass of a dimer (28 kDa). These findings are in good agreement with the size-exclusion data shown in Figure 2 (upper part). A negligible amount of higher-molecular-weight aggregates was reflected by the second peak between 10 and 100 nm, possibly due to unspecific interactions of occludin$^{406–521}$ (Fig. 2, lower part). Comparing the results of the different techniques applied, the coiled-coil domain of occludin apparently preferentially dimerizes.

For claudin-5 colocalization and direct interaction of the full-length protein need to be demonstrated. Fig-

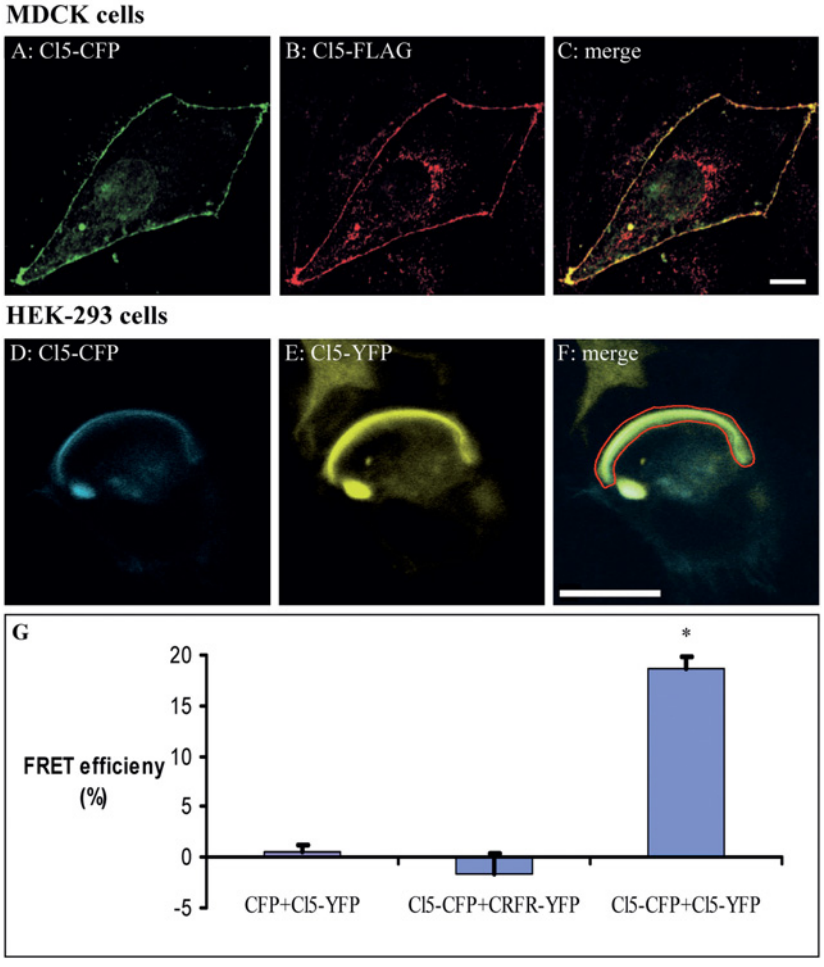

Figure 3. Self-association of claudin-5 in mammalian cells. (*a–c*) Immunostaining of claudin-5 in a MDCK cell cotransfected with claudin-5-CFP (*a*) and claudin-5-FLAG (*b*). Cells were stained with anti-GFP antibodies (green) and mouse anti-FLAG antibodies (red); the merge (*c*) revealed colocalization of claudin-5-CFP and claudin-5-FLAG (yellow) at the plasma membrane of the same cell in a confluent culture. Bar, 10 µm. (*d–f*) Claudin-5-CFP (Cl5-CFP) and claudin-5-YFP (Cl5-YFP) fluorescence signals before photobleaching in living HEK-293 cells cotransfeced with Cl5-CFP and Cl5-YFP. The cell-cell contact area was marked (red) and the respective CFP fluorescence in this area was determined before and after YFP photobleaching. (*g*) FRET from Cl5-CFP to Cl5-YFP, cotransfected in HEK-293 cells, revealed claudin-5 homoassociation within the cell membrane of the same cell. The FRET efficiencies were calculated from HEK-293 cells coexpressing CFP and Cl5-YFP, Cl5-CFP and CRFR-YFP, or Cl5-CFP and Cl5-YFP. The efficiency for Cl5-CFP + Cl5-YFP was significantly higher than that for CFP + Cl5-YFP and claudin-5-CFP + CRFR-YFP, indicating that claudin-5 self-associated within one plasma membrane. Data are means ± SE, n = 20 cells in each group, *p < 0.01 compared to the two other columns.

ure 3a–c exhibits immunostaining of confluent TJ-forming MDCK cells cotransfected with full-length claudin-5-CFP and claudin-5-FLAG, using anti-GFP and anti-FLAG antibodies, respectively. Superposition of the two signals from a cotransfected cell encircled by non-transfected cells demonstrated an overlap of the two claudin-5 molecules in the cell membrane of the same cell.

To investigate whether full-length claudin-5 physically interacts with itself in one membrane, a FRET assay was applied. Figure 3d–f shows fluorescence images of living HEK cells, cotransfected with claudin-5-CFP and claudin-5-YFP. Both fusion proteins were enriched at contacts between two transfected cells, presumably due to a head-to-head interaction between claudins of the two opposing plasma membranes. This contact area was marked (Fig. 3F, encircled by a red line) and used for FRET analysis. The cells were cotransfected with claudin-5-CFP and claudin-5-YFP; as controls we analyzed cotransfections with CFP and claudin-5-YFP, claudin-5-CFP and CRFR-YFP. As shown in Figure 3e, the FRET efficiency for cells coexpressing claudin-5-CFP + claudin-5-YFP (18.6 ± 1.23.7%) was significantly higher than that of those with CFP and claudin-5-YFP (0.5 ± 0.75%), and claudin-5-CFP + CRFR-YFP (–1.6 ± 2.0) ($p > 0.01$, $n = 20$ each, mean ± SE). The data demonstrate a close spatial association of two claudin-5 molecules within one plasma membrane.

To demonstrate that a specific part of claudin-5 is able to interact with itself, the second extracellular loop was examined more closely. Figure 4 (upper part) depicts the size-exclusion chromatography profile of a construct consisting of the second extracellular loop of claudin-5 (claudin-$5^{141–161}$) and MBP. The MBP-fusion protein peaked at its molecular weight of about 45 kDa and at about 90 kDa, corresponding to the monomer and dimer, respectively. Monomer and dimer fractions were identified as claudin-5 loop protein by mass spectrometry (data not shown) and by SDS-PAGE (Coomassie staining: inset, Fig. 4, upper part). Purified MBP did not show any self-association (data not shown). The amount of dimer was concentration dependent as shown in a separate series of experiments. The monomer to dimer ratio rise from about 3 in 1 µM solution to about 6 at 10 nM (Fig. 4, lower part). The dimer formation (using 2 µM loop concentrations) was reduced by the addition of ≥1 mM arginine which also was concentration dependent. Arginine at 400 mM prevented the dimer formation (data not shown). The results show that the second extracellular loop of claudin-5 is able to dimerize and that the dimerization is affected by arginine.

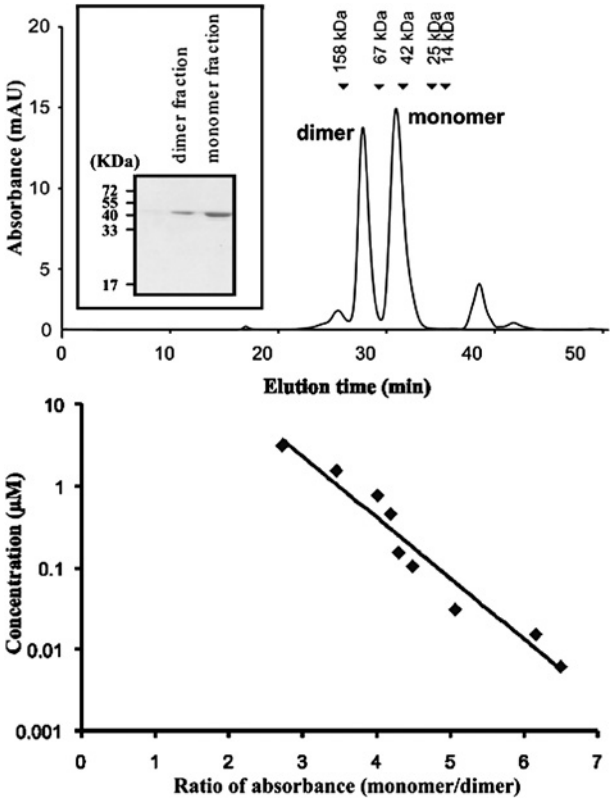

Figure 4. Size-exclusion chromatography of the second extracellular loop of claudin-5 (mouse claudin-$5^{141–161}$) as fusion protein with N-terminal maltose-binding protein (45 kDa). Upper part: selected chromatogram of 0.1 mg/ml MBP-claudin-$5^{141–161}$. Peak fractions of the chromatogram, indicated as dimer and monomer, contained the second extracellular loop (fusion protein) of claudin-5 as verified mass spectrometrically (data not shown) and by SDS-PAGE (Coomassie staining, inset). Arrowheads reveal molecular-weight markers (aldolase, 158 kDa; albumin, 67 kDa; ovalbumin, 42 kDa; chymotrypsinogen A, 25 kDa; ribonuclease, 14 kDa). Lower part: concentration dependence of the dimer formation with MBP-claudin-$5^{141–161}$ as shown by an increasing monomer to dimer ratio with reduction of the protein concentration, using a separate protein preparation. The monomer and dimer amounts were calculated from the respective peak areas.

Discussion

Self-association of TJ proteins and association between different TJ proteins is an absolute prerequisite for the formation of TJs and TJ strands [25]. However, the self-association has not been characterized in detail. Here we show for the first time that the regulatory [26] TJ protein occludin and the strand-forming [27] TJ protein claudin-5 are able to form homodimers in the plasma membrane of the same cell. Furthermore, we were able to identify the domains in both proteins which are responsible for the dimerization. Dimerization has also been postulated for the transmembrane TJ protein JAM [10] as well as for ZO-1 [1, 24], the protein which recruits the above-mentioned TJ proteins. These findings let us assume a dimerization principle within the TJ assembly.

With occludin, we see in TJ-forming MDCK and TJ-free HEK cells, cotransfected with differently tagged occludins, colocalization and coprecipitation, respectively,

of the occludin molecules, indicating self-association of full-length occludin in cells. Colocalization of occludin is observed in the plasma membrane of one cotransfected (CFP-occludin + YFP-occludin) cell even if surrounded by non-transfected cells. This supports the assumption that the occludin-occludin binding detected occurs within the same cell by lateral homoassociation (side-by-side interaction). To further analyze the occludin self-association and to detect an interaction directly within one plasma membrane in living cells, a FRET assay has been established for the first time for TJ proteins. For this assay, TJ-free HEK cells cotransfected with CFP- and YFP-tagged occludin was used and a close spatial association of the two molecules was detectable by energy transfer from CFP of one fusion protein to YFP of an adjacent occludin molecule. FRET typically occurs if the distance of the two fluorophores is ≤6 nm [23]. Thus the FRET signal demonstrates a physical interaction between two occludins in the plasma membrane of a living cell. This excludes interaction between proteins of two opposing plasma membranes, because, in this case, the distance between the CFP- and YFP-tag is too large to result in a FRET signal. Unspecific FRET can be excluded, since cytosolic CFP and YFP or other non-interacting membrane proteins, such as claudin-5-CFP/YFP-aquaporin-1 do not reveal energy transfer. The occludin-occludin interaction appears primarily independent of other TJ proteins, as coprecipitation and FRET is found in cells lacking TJs. An interaction between occludin molecules had already been postulated [3]. However, the latter was based on a peptide-based procedure and so far, there had not been the *in vivo* detection [28].

The interaction area(s) for the self-association of occludin is not clarified. However, our data clearly demonstrate dimerization of the cytosolic C-terminal coiled-coil domain (mouse occludin$^{406–521}$). This domain is remarkably conserved [28] and shows a coiled-coil-helix bundle [24] interacting with helices in other TJ proteins [1]. Size-exclusion chromatography and mass spectrometry indicate the presence of a stable dimer form. Both techniques reveal less monomer than dimer. This is well confirmed by the light-scattering results. The average mass of 23 kDa estimated from static light-scattering data is close to the mass expected for a dimer. The Stokes radius determined is also larger than that of a monomer. A Stokes radius of 1.92 nm would be expected for a protein of globular shape having a mass of 14 kDa by applying the scaling law $R_S(nm) = 0.0557\ M^{0.369}$ [29]. If one calculates the Stokes radius using the above measured average mass of 23 kDa, one gets $R_S = 2.3$ nm. This value is also smaller than the experimentally determined value of 2.86 nm. The larger experimental Stokes radius can be explained by an expanded or elongated structure of the dimer. The assumption of a cylindrical shape of the dimer, therefore, is reasonable, since a cylinder fits well to the predicted [24] coiled-coil domain. Two or more ZO-2 molecules have been claimed to be involved in binding to human occludin$^{404–522}$ [30]. This corresponds to our results that occludin exists and interacts as a dimer. The latter is supported by bioinformatic investigations showing the best matching surface areas if both interacting proteins, e.g. occludin and ZO-1, were modeled as a dimer [24]. Moreover, the dimerizing occludin sequence attracts the SH3-hinge-GuK unit of ZO-1 which also self-associates [1]. We therefore hypothesize that two occludin molecules (occludin homodimer) and two ZO molecules (ZO-1 homodimer) form a heterotetramer. The occludin-ZO-1 interaction is assumed to be responsible for the arrangement of occludin in TJs [31]. In general, the cytosolic C terminus of occludin, which we found dimerized, is highly relevant for its function in TJ assembly, as truncations of that part of occludin affect barrier properties [4]. For claudin-5, dimerization has been suggested by immunoblotting of lysates from human airway epithelium following non-denaturating PFO- as well as SDS-PAGE [32]. We also see claudin-5 dimers isolated from transfected HEK cells in PFO- and SDS-PAGE. However, it is unclear whether this represents the situation in living cells. Using a FRET assay with HEK cells cotransfected with claudin-5-CFP and claudin-5-YFP, a close spatial association of two molecules is detectable by energy transfer from CFP of one claudin to YFP of an adjacent molecule. As TJ-free HEK cells were studied, it is unlikely that the interaction is mediated through other TJ proteins, although traces of ZO-1 can be detected. As ZO-1 dimerizes [24] and associates TJ claudins [7], it could bridge the respective claudins. But here this was impossible because the claudin PDZ-binding C terminus was blocked by the CFP or YFP tag. Unspecific FRET is excluded; cytosolic CFP and claudin-5-YFP or claudin-5-CFP and other YFP-tagged membrane proteins do not transfer energy. This demonstrates specific claudin-5 self-association. In addition, it is clear that the association found takes place within one cell membrane but not between those of two opposing cells. The intracellular lateral interaction (side-by-side interaction) is underlined by electron microscopic freeze-fracture studies of claudin-5 in endothelial cells exhibiting low-nanomolar-sized structures organized as a discontinuous line on the cell surface [*27*]. Similarly, we see discontinuous particles on the exoplasmic membrane face in freeze-fracture replicas of HEK cells transfected with claudin-5 in separate experiments. The small discontinuous extracellular particles are in line with the possibility of small oligomers of claudin-5.

To elucidate the segment of claudin-5 involved in self-association, we constructed an MBP-fusion protein of the second extracellular loop of claudin-5 (mouse claudin-5$^{141–161}$). The loop is able to form a dimer as judged from size-exclusion chromatography. The dimer formation is

concentration dependent in the micro- and submicromolar range and is concentration dependently reduced by the addition of low millimolar arginine, a well-known protein-dissociating agent [33]. Both effects point to a specific interaction. The second extracellular loop contains charged amino acids (R^{145}, E^{146}, K^{157}, E^{159}), and is highly conserved within strand-forming claudins. Charged amino acids in the extracellular loops are thought to be of functional relevance for claudins [28]. With the claudin results, we have demonstrated for the first time that the junction-forming claudin-5 could dimerize within the same cell membrane and that the second extracellular loop can contribute to the association. The two intracellular C termini of a claudin-5 dimer would fit well to a dimer of the cytosolic membrane-associated protein ZO-1. ZO-1 also forms a dimer [1, 24] and, hence, both its PDZ-1 domains might easily associate with the two neighboring C termini of claudin-5 [7]. Thus, we hypothesize that two molecules of claudin-5 (claudin-5 homodimer) and two ZO molecules (ZO-1 homodimer) could build up a heterotetramer. Nevertheless, the data obtained do not exclude that the second extracellular loop of claudin-5 participates in intercellular interaction as well. For the cell-cell interaction, the first extracellular loop seems to be more relevant, as mutations there result in loss of paracellular tightness [34]. Homophilic interactions within TJ strands have been suggested for claudin-1 [35] as well as claudin-3 [36]. Separate size-exclusion chromatography of the second extracellular loop of claudin-3 also reveals dimer formation. Dimerization, therefore, might be a common characteristics of strand-forming claudins.

Finally, homodimers have been identified in JAM-1-transfected ovary cells by means of cross-linking and coimmunoprecipitation [8]. Ultracentrifugation [8] and crystal structural analysis show two salt bridges as a dimerization motif at the extracellular N-terminal loop [10]. This motif is present in all JAMs. The intracellular C-terminal end possesses a classic binding motif for PDZ domains and may interact with PDZ domain 2 or 3 of ZO-1 [8]. We therefore hypothesize that, at the same time, two JAMs (JAM homodimer) and two ZO molecules (ZO-1 homodimer) can form a heterotetramer. JAMs are believed to participate in the development of TJs. Anti-JAM antibodies inhibit paracellular tightness recovery in a transient calcium depletion assay but not in monolayers with well-formed TJs [9]. JAM transfection instead generates the appearance of specific membrane areas in freeze-fracture replicas [37], well-known to occur during the beginning of TJ assembly [28]. Thus, we assume that JAM dimers can also support the arrangement of TJs.

From our measurements and literature data, we conclude that the recruiting protein of junctional structures ZO-1 as well as the transmembrane TJ proteins occludin, claudins, and JAMs exhibit a dimerization potential. This has been demonstrated for ZO-1 [1, 24] and JAM-1 [10], and for claudin-5 and occludin the possibility of a dimerization has been shown by this study. As all the membrane-spanning TJ proteins mentioned bind to ZO-1, we hypothesize that a heterooligomer of transmembrane dimers might function as a common feature within the TJ assembly. The evidence discussed here suggests the following working concept. Occludin is a homodimer which could promote the dimerization of ZO-1. This 'basic unit' of dimers favors recruitment of a claudin homodimer and a JAM homodimer, respectively, which, in turn, would support the organization of higher oligomers and, thus, of the TJ. In addition to the interactions within the same cell, as mainly studied in this paper, one should consider influences of the adherent neighboring cell, which also contributes to the TJ assembly.

Acknowledgements. The authors would like to thank H. Wolburg, Tübingen (Germany) for freeze-fracture electron microscopy, B. Wiesner (Berlin) for support with confocal microscopy and for providing CFP-YFP tandem cDNA, O. Krätke (Berlin) for providing corticotropin-releasing factor receptor 1-YFP cDNA, S. Tsunoda (Berlin) for providing YFP-aquaporin-1 cDNA, and M. Furuse for providing claudin-5 cDNA. This work was supported by DFG BL308/7-1/2.

1 Schmidt A., Utepbergenov D. I., Mueller S. L., Beyermann M., Schneider-Mergener J., Krause G. et al. (2004) Occludin binds to the SH3-hinge-GuK unit of zonula occludens protein 1: potential mechanism of tight junction regulation. Cell. Mol. Life Sci. **61:** 1354–1365
2 Chen Y. H., Merzdorf C., Paul D. L. and Goodenough D. A. (1997) COOH terminus of occludin is required for tight junction barrier function in early *Xenopus* embryos. J. Cell Biol. **138:** 891–899
3 Nusrat A., Chen J. A., Foley C. S., Liand T. W., Tom J., Cromwell M. et al. (2000) The coiled-coil domain of occludin can act to organize structural and functional elements of the epithelial tight junction. J. Biol. Chem. **275:** 29816–29822
4 Balda M. S., Whitney J. A., Flores C., Gonzalez S., Cereijido M. and Matter K. (1996) Functional dissociation of paracellular permeability and transepithelial electrical resistance and disruption of the apical-basolateral intramembrane diffusion barrier by expression of a mutant tight junction membrane protein. J. Cell Biol. **134:** 1031–1049
5 Van Itallie C. M. and Anderson J. M. (1997) Occludin confers adhesiveness when expressed in fibroblasts. J. Cell Sci. **110:** 1113–1121
6 Morita K., Furuse M., Fujimoto K. and Tsukita S. (1999) Claudin multigene family encoding four-transmembrane domain protein components of tight junction strands. Proc. Natl. Acad. Sci. **96:** 511–516
7 Itoh M., Furuse M., Morita K., Kubota K., Saitou M. and Tsukita S. (1999) Direct binding of three tight junction-associated MAGUKs, ZO-1, ZO-2 and ZO-3, with the COOH termini of claudins. J. Cell Biol. **147:** 1351–1363
8 Bazzoni G., Martinez-Estrada O. M., Orsenigo F., Cordenosi M., Citi S. and Dejana E. (2000) Interaction of junctional adhesion molecule with the tight junction components ZO-1, cingulin, and occludin. J. Biol. Chem. **275:** 20520–20526
9 Liu Y., Nusrat A., Schnell F. J., Reaves T. A., Walsh S., Pochet M. et al. (2000) Human junction adhesion molecule regulates tight junction resealing in epithelia. J. Cell Sci. **113:** 2363–2374
10 Kostrewa D., Brockhaus M., D'Arcy A., Dale G. E., Schmid G., Mueller F. et al. (2001) X-ray structure of junctional adhe-

sion molecule: structural basis for homophilic adhesion via a novel dimerisation motif. EMBO J. **20:** 4391–4398
11 Gonzalez-Mariscal L., Betanzos A. and Avila-Flores A. (2000) MAGUK proteins: structure and role in the tight junction. Cell Dev. Biol. **11:** 315–324
12 Fanning A. S., Jameson B. J., Jesaitis L. A. and Anderson J. M. (1998) The tight junction protein ZO-1 establishes a link between the transmembrane protein occludin and the actin cytoskeleton. J. Biol. Chem. **273:** 29745–29753
13 Itoh M., Morita K. and Tsukita S. (1999) Characterization of ZO-2 as a MAGUK family member associated with tight junctions as well as adhaerens junctions with a binding affinity to occludin and alpha-catenin. J. Biol. Chem. **274:** 5981–5986
14 Schmidt A., Utepbergenov D. I., Krause G. and Blasig I. E. (2001) Use of surface plasmon resonance for real-time analysis of the interaction of ZO-1 and occludin. Biochem. Biophys. Res. Commun. **288:** 1194–1199
15 Lowry O. H., Rosebrough N. J., Farr A. L. and Randall R. J. (1951) Protein measurement with the folin phenol reagent. J. Cell Biol. **193:** 265–275
16 Andreeva A. Y., Krause E., Muller E. C., Blasig I. E. and Utepbergenov D. I. (2001) Protein kinase C regulates the phosphorylation and cellular localization of occludin. J. Biol. Chem. **276:** 38480–38486
17 Karpova T. S., Baumann C. T., He L., Wu X., Grammer A., Lipsky P. et al. (2003) Fluorescence resonance energy transfer from cyan to yellow fluorescent protein detected by acceptor photobleaching using confocal microscopy and a single laser. J. Microsc. **209:** 56–70
18 Gao J., Yu H., Song Q. and Li X. (2005) Establishment of HEK293 cell line expressing green fluorescent protein-aquaporin-1 to determine osmotic water permeability. Anal. Biochem. **342:** 53–58
19 Heinrich N., Meyer M. R., Furkert J., Sasse A., Beyermann M., Bonigk W. et al. (1998) Corticotropin-releasing factor (CRF) agonists stimulate testosterone production in mouse leydig cells through CRF receptor-1. Endocrinology **139:** 651–658
20 Tsunoda S. P., Wiesner B., Lorenz D., Rosenthal W. and Pohl P. (2004) Aquaporin-1, nothing but a water channel. J. Biol. Chem. **279:** 11364–11367
21 Gast K., Noppert A., MullerFrohne M., Zirwer D. and Damaschun G. (1997) Stopped flow dynamic light scattering as a method to monitor compaction during protein folding. Eur. Biophys. J. **25:** 211–219
22 Provencher S. W. (1982) Contin – a general-purpose constrained regularization program for inverting noisy linear algebraic and integral-equations. Comp. Phys. Commun. **27:** 229–242
23 Sekar R. B. and Periasamy A. (2003) Fluorescence resonance energy transfer (FRET) microscopy imaging of live cell protein localizations. J. Cell Biol. **160:** 629–633
24 Muller S. L., Portwich M., Schmidt A., Utepbergenov D. I., Huber O., Blasig I. E. et al. (2005) The tight junction protein occludin and the adherens junction protein alpha-catenin share a common interaction mechanism with ZO-1. J. Biol. Chem. **280:** 3747–3756
25 Tsukita S., Furuse M. and Itoh M. (2001) Multifunctional strands in tight junctions. Nat. Rev. Mol. Cell Biol. **2:** 285–293
26 Sakakibara A., Furuse M., Saitou M., Ando-Akatsuka Y. and Tsukita S. (1997) Possible involvement of phosphorylation of occludin in tight junction formation. J. Cell Biol. **137:** 1393–1401
27 Morita K., Sasaki H., Furuse M. and Tsukita S. (1999) Endothelial claudin: claudin-5/TMVCF constitutes tight junction strands in endothelial cells. J. Cell Biol. **147:** 185–194
28 Gonzales-Mariscal L., Betanzos A., Nava P. and Jaramillo B. E. (2003) Tight junction proteins. Progr. Biophys. Mol. Biol. **81:** 1–44
29 Uversky V. N. (1993) Use of fast protein size-exclusion liquid-chromatography to study the unfolding of proteins which denature through the molten globule. Biochemistry **32:** 13288–13298
30 Peng B. H., Lee J. C. and Campbell G. A. (2003) *In vitro* protein complex formation with cytoskeleton-anchoring domain of occludin identified by limited proteolysis. J. Biol. Chem. **278:** 49644–49651
31 Matter K. and Balda M. S. (1998) Biogenesis of tight junctions: the C-terminal domain of occludin mediates basolateral targeting. J. Cell Sci. **111:** 511–519
32 Coyne C. B., Gambling T. M., Boucher R. C., Carson J. L. and Johnson L. G. (2003) Role of claudin interactions in airway tight junctional permeability. Am. J. Physiol. Cell. Mol. Physiol. **285:** L1166–L1178
33 Tsumoto K., Umetsu M., Kumagai I., Ejima D., Philo J. S. and Arakawa T. (2004) Role of arginine in protein refolding, solubilization, and purification. Biotechnol. Prog. **20:** 1301–1308
34 Wen H., Watry D. D., Marcondes M. C. G. and Fox H. S. (2004) Selective decrease in paracellular conductance of tight junctions: role of the first extracellular domain of claudin-5. Mol. Biol. Cell **24:** 8408–8417
35 McCarthy K. M., Francis S. A., McCormack J. M., Lai J., Rogers R. A., Skare I. B. et al. (2000) Inducible expression of claudin-1-myc but not occludin-VSV-G results in aberrant tight junction strand formation in MDCK cells. J. Cell Sci. **113:** 3387–3398
36 Furuse M., Sasaki H. and Tsukita S. (1999) Manner of interaction of heterogeneous claudin species within and between tight junctions. J. Cell Biol. **147:** 891–903
37 Itoh M., Sasaki H., Furuse M., Ozaki H., Kita T. and Tsukita S. (2001) Junctional adhesion molecule (JAM) binds to PAR-3: a possible mechanism for the recruitment of PAR-3 to tight junctions. J. Cell Biol. **154:** 491–497


To access this journal online:
http://www.birkhauser.ch